Optical refractometer based on a birefringent Bragg grating written in an H-shaped fiber

O. Frazão,[1,*] T. Martynkien,[2] J. M. Baptista,[1] J. L. Santos,[1] W. Urbanczyk,[2] and J. Wojcik[3]

[1]*INESC Porto, Rua do Campo Alegre 687, 4169-007, Porto, Portugal*
[2]*Wroclaw University of Technology, 50-370 Wroclaw, Wybrzeze Wyspianskiego 27, Poland*
[3]*Maria Curie-Skłodowska University, Lublin 20-031 Poland*
[*]*Corresponding author: ofrazao@inescporto.pt*

Received September 29, 2008; accepted October 30, 2008;
posted November 25, 2008 (Doc. ID 102213); published December 24, 2008

An optical refractometer based on a birefringent (Hi-Bi) fiber Bragg grating (FBG) written in a new H-shaped fiber structure is proposed. This structure is formed by opening the two holes of a side-hole fiber using chemical etching. When the Hi-Bi FBG is immersed in different liquids, different responses of the slow and fast wavelengths are obtained. The refractometer is also capable of simultaneous measurement of refractive index and temperature. © 2008 Optical Society of America

OCIS codes: 060.2310, 060.3735, 060.2370.

The fiber Bragg grating (FBG) is an intrinsic optical fiber sensor that offers numerous advantages over electric transducers owing to its wavelength-encoded operation, high sensitivity, immunity to electromagnetic interference, small size, and compatibility to multipoint measurement over large distances with negligible signal degradation [1].

FBG structures used in refractometric configurations have been previously studied. The first demonstration of an FBG as a refractometer was done in 1998 by Asseh *et al.* [2], and it was based on the application of chemical etching to the fiber region where the FBG was located. Several other authors have also studied this type of refractometer. Pereira *et al.* [3] proposed a FBG sensing system for simultaneous measurement of salinity and temperature. Iadicicco *et al.* [4] studied the FBG sensitivity to liquid refractive indexes as a function of the fiber cladding diameter after the etching process. Liang *et al.* [5] demonstrated two types of FBG-based refractometric sensors. The first device is an FBG in an etched fiber with a diameter of 6 μm; the second sensing head is a 3-μm-diameter fiber Fabry–Perot interferometer (FFPI) with FBG mirrors. When the two devices are compared, the narrow fringes of the FFPI-channeled spectrum permitted a higher sensitivity compared with the basic FBG refractometer. In another work, Iadicicco *et al.* [6] proposed a new FFPI refractometer where only a small length of the cladding layer of the FBG region was etched. In this case, it is the narrow transmission band in the FBG envelope that is sensitive to the external refractive index. FBG-based refractive index sensors with temperature referentiation were also reported by Liang *et al.* [7]. In 2001, Schroeder *et al.* [8] developed a FBG side-polishing technology for refractometry. The fiber cladding was partly removed by side polishing, and the FBG was exposed to a liquid via the evanescent field interaction of the guided fiber mode. This refractometer was also compensated in temperature using another FBG located in the unpolished region. An optical chemical sensor based on an etched D-fiber FBG with potential for temperature compensation was proposed by Zhou *et al.* [9]. Recently, optical refractometers based on photonic crystal fibers were proposed by Huy *et al.* [10].

In this Letter, a new FBG refractometer based on an H-shaped fiber is proposed. The H-shaped fiber is formed by exposing Hi-Bi side-hole fiber to chemical etching. The two holes of the side-hole fiber are open, allowing the evanescent field of the Hi-Bi FBG to interact with the external liquid. Owing to the birefringence of this sensing structure, it is possible to simultaneously measure refractive index and temperature. Alternatively, using the differential readout of two resonant wavelengths of the Hi-Bi FBG, it is possible to measure a refractive index of liquid with very small temperature cross sensitivity.

In the experimental set-up shown in Fig. 1, the sensing head was illuminated with an erbium-doped broadband source (3 mW), and its reflection spectrum was monitored using an optical spectrum analyzer (OSA). The side-hole fiber used in the experiments has an elliptical core of dimensions of 6.3 $\times$ 2.5 μm, a cladding with 125 μm diameter, and an acrylate coating jacket. The difference of refractive index between 20 mol.% germanium-doped core and nondoped silica cladding is 0.0264 at the wavelength of 633 nm. A FBG was inscribed using a 10-mm-long uniform phase mask and a KrF excimer laser operating at 248 nm, with a pulse power of 300 mJ cm^{-2} and a repetition rate of 20 Hz. Owing to the fiber birefringence, two reflection peaks were obtained with the wavelengths of 1566.64 nm (fast axis grating, λ_f) and 1567.85 nm (slow axis grating, λ_s). After FBG inscription, chemical etching was applied. All the FBG region was immersed inside an aqueous solution of

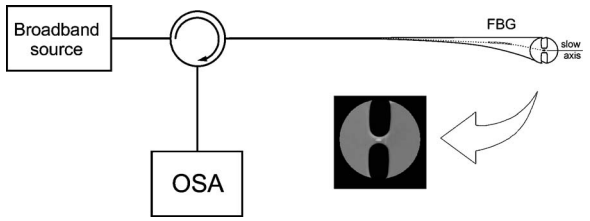

Fig. 1. Experimental setup of the FBG refractometer based on an H-shaped fiber.

hydrofluoric acid (HF 40%), yielding a diameter cladding reduction rate of ~1.5 μm/min. The etching process was monitored by analyzing the FBG spectral response, and it was stopped when the holes of the side-hole fiber were open and an H-shaped fiber was formed. The positions of Bragg peaks changed, when the evanescent field was able to overlap with the fluid. The etching process lasted approximately 9 min, which resulted in opening the holes and reducing the cladding diameter of the side-hole fiber. Figure 2 shows the spectral response of FBG before and after etching process. It is observed in Fig. 2(a) that after completion of the etching process, the amplitude of the FBG spectrum decreases, but the separation between the two polarizations-related resonances increases, which indicates that the fiber birefringence increases after the etching process. This effect is related to reduction of the thickness of the glass bridge that contains the core. On the other hand, Fig. 2(b) presents the spectral response of the Hi-Bi FBG after etching when the structure is surrounded by air and water. When the fiber is surrounded by air, the contrast of refractive index between the cladding region and the holes (air) is higher, and therefore the fiber birefringence is higher. When the fiber is surrounded by water, the refractive index contrast is reduced, which lowers the fiber birefringence and in consequence reduces separation between the two polarization-related resonances. Table 1 summarizes the values of the fiber birefringence for several situations.

The refractometer based on the H-shaped fiber was tested in measurements of refractive index of liquid in the interval [1.34, 1.39]. Figure 3(a) shows the associated wavelengths shifts of the FBG resonances, which follow linear dependences with coefficients 0.2 nm/refractive-index unit (RIU) (fast axis grating) and 0.14 nm/RIU (slow axis grating). These resonances have different sensitivities, because the overlap of the modal field with liquid depends on the mode polarization. Figure 3(b) presents the variation of the difference in resonance wavelengths and the fiber birefringence with the liquid refractive index. The results reflect the effect of increase of effective indices of both polarization modes with the increase of the liquid refractive index. From the data presented, the dependences of the difference in resonance wavelengths and the fiber birefringence are linear with coefficients of −0.97 nm/RIU and -9×10^{-4} RIU^{-1}, respectively.

Table 1. Birefringence of the Side-Hole and H-Shaped Fibers

	Δλ (nm)	B ($\times 10^{-4}$)
Side-hole fiber (before etching)	0.44	4.07
H-shaped fiber (air)	0.54	5.00
H-shaped fiber (water)	0.46	4.26

The Hi-Bi FBG in the H-shaped fiber was also characterized against temperature. The refractometer was immersed in water and heated in the range from 25°C up to 65°C. As Fig. 4(a) shows, the two polarized-related grating resonances have similar temperature sensitivities, with coefficients of 10.67 pm/°C (fast axis grating) and 10.97 pm/°C (slow axis grating). Figure 4(b) shows the temperature dependence of the resonance wavelength difference and the fiber birefringence, from which we obtained the coefficients of 0.2 pm/°C and 2×10^{-7}°C^{-1}, respectively. The response of the grating to temperature is due to combination of two effects: one is the increase of the refractive index of the glass (dominant), while the other is the decrease of the water refractive index with the temperature (secondary). The birefringence variation with temperature in the H-shaped fiber is small when compared with the

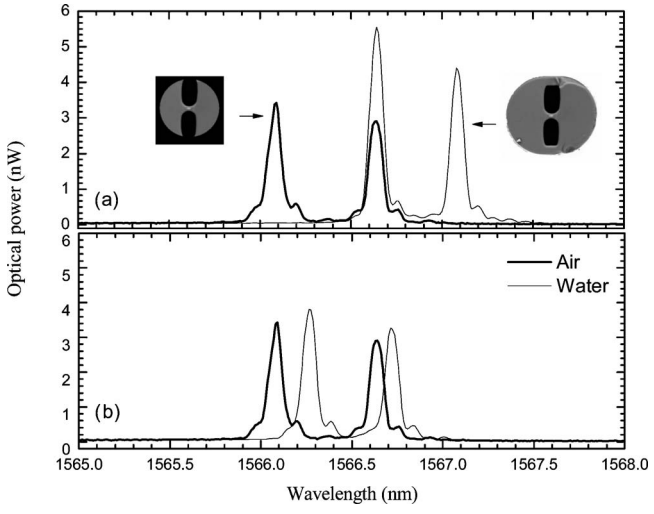

Fig. 2. (a) Spectral response of the Hi-Bi FBG before and after chemical etching, (b) FBG spectrum when the sensing head was surrounded by air and water.

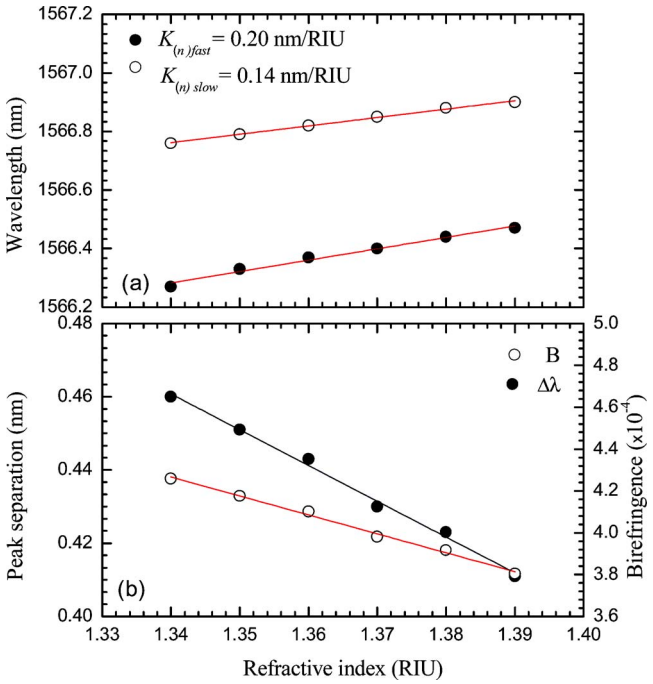

Fig. 3. (Color online) Dependence with the liquid refractive index of (a) wavelength of the two resonances of the birefringent FBG and (b) resonance wavelength difference and grating birefringence.

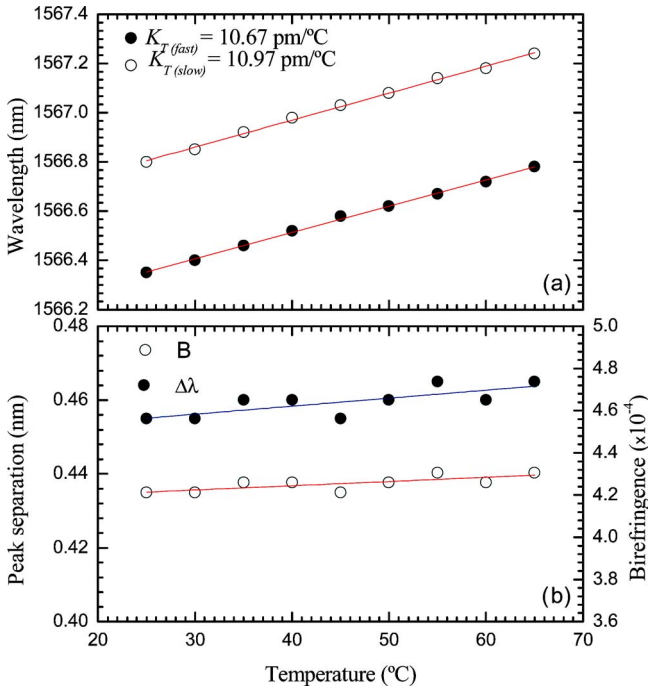

Fig. 4. (Color online) Dependence with temperature of (a) wavelength of the two resonances of the birefringent FBG and (b) resonance wavelength difference and grating birefringence.

variation of the birefringence with the refractive index of liquid. Therefore, for small temperature variations, the difference in resonance wavelengths can approximately be considered as temperature independent.

From the level of data scattering at constant temperature shown in Fig. 3, we estimate the resolution of refractive index measurement at 3×10^{-3} RIU.

Using the proposed sensing element, it is also possible to simultaneously measure the refractive index of liquid and its temperature. Indeed, a matrix equation for ΔT and Δn can be written as follows (coefficients identified in Fig. 3 and 4):

$$\begin{bmatrix} \Delta T \\ \Delta n \end{bmatrix} = \frac{1}{K_{(T)f}K_{(n)s} - K_{(n)f}K_{(T)s}} \begin{bmatrix} K_{(n)s} & -K_{(n)f} \\ -K_{(T)s} & K_{(T)f} \end{bmatrix} \begin{bmatrix} \Delta\lambda_f \\ \Delta\lambda_s \end{bmatrix}. \quad (1)$$

From the sensitivity coefficients given in those figures, the above equation can be written as

$$\begin{bmatrix} \Delta T \\ \Delta n \end{bmatrix} = \frac{1}{0.7 \times 10^{-3}} \begin{bmatrix} 0.14 & -0,2 \\ -10.97 & 10.67 \end{bmatrix} \begin{bmatrix} \Delta\lambda_f \\ \Delta\lambda_s \end{bmatrix}. \quad (2)$$

The system performance was evaluated when the sensing element was exposed simultaneously to refractive index and temperature changes. From the results shown in Fig. 5, we estimated the resolution of two-parameter measurements at ±0.005 RIU and ±1.6°C, respectively for refractive index and temperature. Work is ongoing concerning the optimization of the H-shaped fiber design to further improve the measurement resolution.

In conclusion, a new refractometer based on an Hi-Bi FBG written in an H-shaped fiber was presented. The H-shaped fiber was obtained by subjecting the side-hole fiber to chemical etching. With this process the holes were opened, permitting physical contact of the surrounding liquid with the internal fiber region. This sensing element was first tested in refractive index measurements. Very low temperature cross sensitivity was demonstrated for the differential readout of the Bragg wavelengths corresponding to the orthogonally polarized fundamental modes. Application of the sensing element for simultaneous measurement of refractive index and temperature was also proposed.

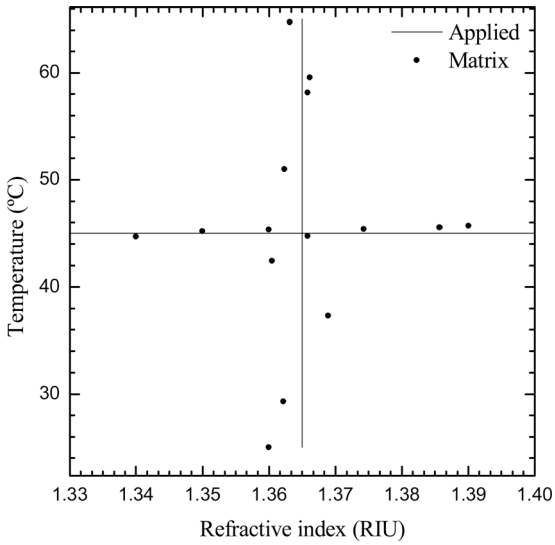

Fig. 5. (Color online) Sensor output as determined by Eq. (2) for liquid refractive index change at constant temperature and temperature change at constant refractive index.

This work was performed in the framework of European Program COST, Action 299 "Optical Fibers for New Challenges Facing the Information Society."

References

1. A. D. Kersey, M. A. Davis, H. J. Patrick, M. LeBlanc, K. P. Koo, C. G. Askins, M. A. Putnam, and E. J. Friebele, J. Lightwave Technol. **15**, 1442 (1997).
2. A. Asseh, S. Sandgren, H. Ahlfeld, B. Sahlgren, R. Stubbe, and G. Edwall, Fiber Integr. Opt. **17**, 51 (1998).
3. D. A. Pereira, O. Frazao, and J. L. Santos, Opt. Eng. (Bellingham) **43**, 299 (2004).
4. A. Iadicicco, A. Cusano, A. Cutolo, R. Bernini, and M. Giordano, IEEE Photonics Technol. Lett. **16**, 1149 (2004).
5. W. Liang, Y. Huang, Y. Xu, R. K. Lee, and A. Yariv, Appl. Phys. Lett. **86**, 151122 (2005).
6. A. Iadicicco, A. Cusano, S. Campopiano, A. Cutolo, and M. Giodano, IEEE Sens. J. **5**, 1288 (2005).
7. X. Sang, C. Yu, T. Mayteevarunyoo, K. Wang, Q. Zhang, and P. L. Chu, Sens. Actuators B **120**, 754 (2007).
8. K. Schroeder, W. Ecke, R. Mueller, R. Willsch, and A. Andreev, Meas. Sci. Technol. **12**, 757 (2001).
9. K. Zhou, X. Chen, L. Zhang, and I. Bennion, Electron. Lett. **40**, 232 (2004).
10. M. C. P. Huy, G. Laffont, Y. Frigna, V. Dewynter-Marty, P. Ferdinand, P. Roy, J.-M. Blondy, D. Pagnoux, W. Blanc, and B. Dussardier, Meas. Sci. Technol. **17**, 992 (2006).